Available online at www.sciencedirect.com
ScienceDirect
Trans. Nonferrous Met. Soc. China 34(2024) 283−297
Transactions of Nonferrous Metals Society of China
www.tnmsc.cn

Advancements on chemical−biological dissolution mechanism and leaching kinetics of chalcocite

Chao-jun FANG[1,2,3], Jun WANG[4,5], Guan-zhou QIU[4,5]

1. College of Chemistry and Chemical Engineering, Henan Polytechnic University, Jiaozuo 454000, China;
2. Collaborative Innovation Center of Coal Work Safety and Clean High Efficiency Utilization, Henan Polytechnic University, Jiaozuo 454000, China;
3. State Key Laboratory of Complex Nonferrous Metal Resources Clean Utilization, Kunming University of Science and Technology, Kunming 650093, China;
4. School of Minerals Processing and Bioengineering, Central South University, Changsha 410083, China;
5. Key Lab of Bio-hydrometallurgy of Ministry of Education, Central South University, Changsha 410083, China

Received 5 September 2022; accepted 18 May 2023

Abstract: Chalcocite is one of the most industrially valuable copper-bearing minerals available for bioleaching. However, the efficiency of chalcocite bioleaching remains unsatisfactory. To better understand the bioleaching process of chalcocite, researches on chemical−biological dissolution mechanisms and leaching kinetics are reviewed. The crystal structure of chalcocite is systematically characterized. The mechanisms for chemical dissolution, electrochemical dissolution, and biological dissolution are summarized and elaborated. The effects of leaching parameters on the leaching kinetics are discussed, and issues in industrial-scale bioleaching are identified. However, the fine leaching process and leaching mechanism of chalcocite still require further study. New research techniques, including synchrotron radiation-based measurements, can be employed to determine the fine mechanism for chalcocite dissolution with interdisciplinary chemistry−biology studies, which may enable efficient extraction of copper from chalcocite in the future.

Key words: chalcocite; bioleaching; dissolution mechanism; kinetics; synchrotron radiation

1 Introduction

Copper is one of the most important nonferrous metals, and it has widespread applications in the electrical industry, light industry, machinery manufacturing, construction industry, and national defense industry [1]. Currently, the majority of copper is recovered from copper-bearing ores, the most valuable of which are copper sulfide ores [2].

Generally, copper is extracted from copper sulfide by the beneficiation−pyrometallurgical process. However, this process has drawbacks, including a long process time, high cost, significant pollution, and environmental unfriendliness [3,4]. As one of the advanced technologies for clean utilization of copper sulfide minerals, bioleaching exhibits simple operation, low cost, and environmental friendliness [5−8]. It has been successfully applied to the treatment of various low-grade mineral resources and has become an important research area in mineral processing and metallurgy [9−12].

Chalcocite (Cu_2S) has a copper content of 79.86% and is one of the most industrially valuable copper-bearing minerals available for bioleaching.

Corresponding author: Jun WANG, Tel: +86-731-88879622, E-mail: wjwq2000@126.com
DOI: 10.1016/S1003-6326(23)66398-8

Due to the complexity of mineralization, chalcocite typically occurs in copper-rich and sulfur-poor mesothermal hydrothermal deposits or in the lower oxidation zones of copper sulfide deposits. In addition, chalcocite is commonly associated with pyrite, chalcopyrite, bornite and other sulfide minerals [13,14].

The bioleaching process of chalcocite has been researched for decades. Chile pioneered the heap leaching−extraction−electrowinning process for chalcocite [15], and numerous chalcocite mines achieved the industrial practice of chalcocite bioleaching since then. However, even after decades of research and practice, there are still issues, including low copper extraction, low leaching rates, and inefficient resource utilization.

Therefore, this work is focused on the chemical−biological leaching mechanism and leaching kinetics of chalcocite based on its crystal structure. In particular, the application of synchrotron radiation-based methods to determine the chemical−biological leaching mechanism of copper sulfide minerals is reviewed, which may refine the leaching mechanisms and improve the efficiency of chalcocite leaching.

2 Crystal structure of chalcocite

The crystal structure of chalcocite is intricate. High chalcocite is classified into the $P_{6\text{-}3}/mmc$ space group, where S atoms are most tightly packed in hexagons, and di-coordinated, tri-coordinated, and tetra-coordinated Cu atoms randomly fill the gaps among S atoms [16]. The crystal structure of low chalcocite is derived from that of high chalcocite; it is monoclinic but differs from that of high chalcocite. By investigating the crystal structures of djurleite and low chalcocite, EVANS [17] found that the crystal structure of low chalcocite may belong to the Pc space group rather than the $P_{2\text{-}1}/c$ space group as previously reported. The crystal structure of djurleite is similar to that of low chalcocite and belongs to the monoclinic system and $P_{2\text{-}1}/n$ space group. There are 62 different Cu atoms in the djurleite crystal structure, of which 52 are in threefold, triangular coordination with sulfur, nine in tetrahedral, and one in linear coordination. In addition, the tetrahedral, triangular and linear Cu—S bonds in low chalcocite and djurleite exhibit large variations in bond length compared with the crystal structures of other copper-rich sulfides [18]. The crystal structures of high chalcocite, low chalcocite, djurleite, and digenite are shown in Fig. 1.

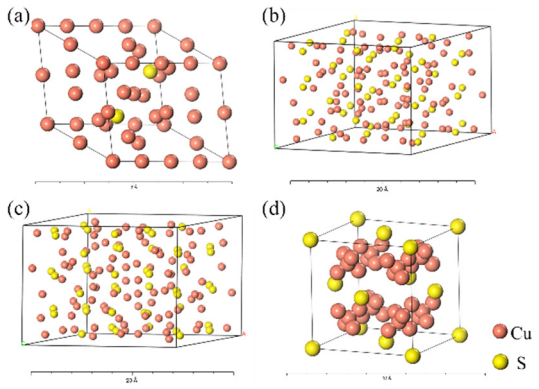

Fig. 1 Crystal structures of high chalcocite (a), low chalcocite (b), djurleite (c), and digenite (d) [19,20]

It can be seen from Fig. 1 that high chalcocite is present in the hexagonal system, and the copper atoms are mainly combined with the sulfur atoms via tri-coordination, tetra-coordination and hexa-coordination. However, there are 48 S atoms and 96 Cu atoms in the low chalcocite cell, with lattice parameters of a=15.246 Å, b=11.884 Å, c=13.494 Å, $\alpha=\gamma$=90°, and β=116.35°.

The oxidative dissolution properties of minerals are determined by their crystal structures. For copper−sulfur compounds, the Cu—S bond length increases with increasing copper-to-sulfur ratios, and the bond energy decreases accordingly. Chalcocite has long Cu—S bonds and low bond energies, which facilitates the dissolution. In addition, chalcocite is a P-type semiconductor with a forbidden bandwidth of approximately 1.8 eV, and charge transfer occurs during leaching through holes at the solution interface and through the valence band of the mineral [21].

When chalcocite is in a solution containing Fe^{3+}/Fe^{2+} pairs, the band structure of chalcocite bends downward at the solid/liquid interface, while crystalline Cu^{+} is oxidized to Cu^{2+} and dissolved, and the S^{2-} is oxidized to S_2^{2-}. In this process, copper is extracted from the chalcocite, and no S^0 is generated [22].

In the early stage of chalcocite dissolution, a fracture model of valence bonds in the mineral crystals can be proposed, as shown in Reactions (1)−(3) [23]:

$$Cu^{+}(crystal)-e\rightarrow Cu^{2+}(aq) \quad (1)$$

$$S^{2-}(crystal)-e\rightarrow 0.5\,S_2^{2-}(crystal) \quad (2)$$

$$Cu^{+}(crystal)+0.5\,S_2^{2-}(crystal)\rightarrow 0.5(Cu^{+})_2\,S_2^{2-}(crystal) \quad (3)$$

Disruption of the valence bond structure in the chalcocite crystal upon oxidation and electron loss is well explained in this model. The crystalline Cu^{+} is oxidized to Cu^{2+}, and S^{2-} is oxidized to S_2^{2-}; then, the generated S_2^{2-} combines with Cu^{+} to form CuS ($(Cu^{+})_2\,S_2^{2-}$) due to the high migration rate of Cu^{+} in chalcocite crystal.

3 Dissolution mechanism of chalcocite

3.1 Chemical dissolution mechanism of chalcocite

Chalcocite is soluble in oxygenated acid solutions, and the leaching efficiency is significantly improved by the addition of Fe^{3+}. However, the process of chalcocite dissolution can be divided into two distinct stages regardless of the presence of Fe^{3+} [24−28]. Reactions (4)−(8) show the chemical reactions occurring during chalcocite dissolution:

$$2Cu_2S+O_2+4H^{+}\rightarrow 2CuS+2Cu^{2+}+2H_2O \quad (4)$$

$$2CuS+O_2+4H^{+}\rightarrow 2S^{0}+2Cu^{2+}+2H_2O \quad (5)$$

$$Cu_2S+2Fe^{3+}\rightarrow CuS+Cu^{2+}+2Fe^{2+} \quad (6)$$

$$CuS+2Fe^{3+}\rightarrow S^{0}+Cu^{2+}+2Fe^{2+} \quad (7)$$

$$4Fe^{2+}+O_2+4H^{+}\rightarrow 4Fe^{3+}+2H_2O \quad (8)$$

Chalcocite is oxidized to covellite in the first stage (Reaction (4) or (6)), and the generated covellite is further oxidized to S^0 in the second stage (Reaction (5) or (7)). In this process, copper is continuously dissolved and extracted. In addition, sufficient dissolved oxygen and H^{+} are essential when using Fe^{3+} as the oxidant (Reaction (8)).

According to the chemical oxidation model for sulfide minerals [29], second stage leaching of chalcocite, as with leaching of covellite, follows the polysulfide dissolution pathway. S is oxidized along the polysulfide−S^0 pathway, while Cu is oxidized to Cu^{2+} and gradually dissolved. As early as the 1930s, S^0 was discovered during chemical leaching of covellite [25].

The first stage of chalcocite leaching is significantly different from the second stage. There is not just one simple chemical reaction as expressed by Reaction (4) or (6), but a series of complex chemical reactions involving various intermediates. WHITESIDE and GOBLE [30] proposed a phase transformation order of first stage leaching chalcocite, chalcocite (Cu_2S) → djurleite ($Cu_{1.97}S$) → digenite ($Cu_{1.8}S$) → anilite ($Cu_{1.75}S$) → geerite ($Cu_{1.6}S$) → spionkopite ($Cu_{1.4}S$) → yarrowite ($Cu_{1.125}S$) → covellite (CuS). According to the stoichiometry, when the level of copper extraction reaches 10%, 20%, 30%, or 50%, chalcocite is transformed into digenite, geerite, spionkopite, or covellite.

However, the actual dissolution process of chalcocite is complex. Due to the irregularity of the crystals and the inhomogeneity of the particle sizes, the leaching rates of different particles are not synchronized, and various intermediates coexist and interact with each other. Therefore, it is inaccurate to speculate on the intermediates simply by copper extraction.

HASHEMZADEH and LIU [31] investigated the evolution of surface properties during chloride leaching of chalcocite and reported that sulfur was transformed sequentially from monosulfide S^{2-} to disulfide S_2^{2-}, polysulfide S_n^{2-} and elemental sulfur S^0. At a high solution potential, there was only a small amount of S^0 on the mineral surface, and copper extraction was not improved by removing S^0 through washing with CS_2. Conversely, at a low solution potential, a slight increase in the copper extraction was associated with the removal of sulfur from the mineral surface.

Therefore, it is proposed that the leaching process was controlled by the slow decomposition of polysulfides at a high solution potential, whereas it was controlled by diffusion of the S^0 layer and slow decomposition of the polysulfides at a lower solution potential. Therefore, a dissolution mechanism for chalcocite was proposed, as shown in Fig. 2.

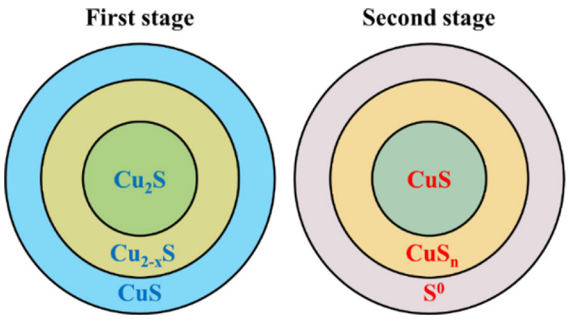

Fig. 2 Model for chalcocite dissolution mechanism [31]

In addition, chalcocite seldom occurs alone but is frequently associated with other minerals in natural ores. HIDALGO et al [32] investigated the mineral replacement reaction between coarse-grained natural bornite−chalcocite in an acidic solution without oxidizers at 90 °C. It was found that the transformations followed a three-stage reaction sequence for bornite and a one-stage reaction sequence for chalcocite. The chalcocite and bornite present in the unreacted samples were converted into digenite with layered displacement texture features. Finally, all of the phases were replaced by covellite, which was accompanied by the formation of pores. TORRES et al [33] found that the dissolution rate of chalcocite was significantly accelerated in a short period of time by adding MnO_2 to brine, and the effect of the H_2SO_4 concentration was insignificant when leaching at high chloride and MnO_2 concentrations. Within 48 h, 71% of the copper was extracted from chalcocite with reject brine, 100 mg of MnO_2 per 200 g of material, and 0.5 mol/L H_2SO_4.

3.2 Electrochemical dissolution mechanism of chalcocite

Ferric ions and the redox potential have important influences on the electrochemical dissolution of chalcocite. It has been reported that the kinetics of the first stage was controlled by diffusion or chemical reactions. The leaching process was dominated by ferric ion diffusion at lower ferric concentrations (less than 0.058 mol/L), whereas it was controlled by the anodic electrochemical dissolution mechanism at higher ferric ion concentrations (greater than 0.058 mol/L) [34]. However, although the first stage of chalcocite leaching was not sensitive to the redox potential, the second stage was strongly affected by the redox potential. The leaching rate of covellite at 839 mV (vs SHE) was not much different from that at 889 mV (vs SHE), but when the redox potential was reduced to 789 mV (vs SHE), the leaching rate significantly decreased [26]. Furthermore, the anodic electrochemical dissolution mechanism of chalcocite was not affected by the leaching temperature, and increasing the leaching temperature accelerated only the leaching kinetics. Therefore, the dissolution of chalcocite and covellite followed an electrochemical mechanism, and the dissolution rate was adjusted by controlling the redox potential.

ARCE and GONZÁLEZ [35] studied the dissolution behavior of chalcocite with cyclic voltammetry in a sulfuric acid leaching system and found that the anode products on the surface were subject to oxidation potential. The oxidation product was djurleite ($Cu_{1.92}S$) when the potential was less than 423 mV (vs SHE), while it was digenite ($Cu_{1.6}S$) when the potential was raised to 423−573 mV (vs SHE). However, blue-remaining covellite ($Cu_{1.40-1.36}S$) and covellite (CuS) were generated once the potential exceeded 573 mV (vs SHE). By studying the anodic polarization curve of chalcocite in a sulfuric acid leaching system, ELSHERIEF et al [36] found that the insoluble intermediate $Cu_{2-x}S$, produced by chalcocite during anodic oxidation, was the major barrier for leaching of chalcocite. By investigating the electrochemical steady-state polarization parameters, BOLORUNDURO [24] suggested that CuS and S^0 served as passivation substances during the electrochemical dissolution of chalcocite and that the activity of crystalline Cu^+ was the primary factor affecting the leaching rates of chalcocite and covellite.

WEN [37] researched the electrochemical dissolution process of chalcocite with cyclic voltammetry. The addition of leaching micro-organisms significantly improved the dissolution rate of chalcocite, and the effect of sulfur-oxidizing bacteria was greater than that of iron-oxidizing bacteria. Moreover, the temperature had an important effect on the electrochemical dissolution of chalcocite. At room temperature, there was only one oxidation peak on the cyclic voltammetry curve for chalcocite sulfuric acid leaching, which corresponded to the electrochemical oxidation of chalcocite to S^0. However, two oxidation peaks were obtained when the temperature was increased, and a series of intermediates, including djurleite, digenite, and covellite, were generated. WU et al [38] found that the pH and temperature had significant effects on the corrosion current and corrosion potential of chalcocite. The Gibbs free energy of the chemical reaction decreased with decreasing pH and increasing temperature, which increased the anodic corrosion current density and promoted the electrochemical corrosion reaction of chalcocite.

Furthermore, the electrochemical behavior of chalcocite under different oxidizing atmospheres

has been reported. Using an analysis of the Cu L-edge and O K-edge absorption spectra, TODD and SHERMAN [39] investigated the surface oxidation process of chalcocite in air and leaching solutions with pH of 2−11. The results showed that the surface oxidation product of chalcocite was Cu_2O at low pH levels, but as the leaching pH increased, the oxidation products gradually changed to CuO and $CuSO_4$. Using an experimental platform combining an electrochemical workstation and surface detection, VELÁSQUEZ et al [40] made in-situ detection of the surface products at different redox potentials. On this platform, CuO, $Cu(OH)_2$, and $Cu_3(SO_4)(OH)_4$ were detected on the surface after a specific potential was applied. ARCE and GONZÁLEZ [35] compared the electrochemical behavior of chalcocite, chalcopyrite and bornite in sulfuric acid solutions; the non-stoichiometric sulfide $Cu_{n-1}Fe_{n-1}S_{2n}$, rather than covellite, was found to be the intermediate of chalcopyrite, and the reduction intermediate of chalcopyrite was chalcocite rather than bornite.

3.3 Biological dissolution mechanism of chalcocite

The direct and indirect mechanisms are used to indicate how microorganisms promote the dissolution of chalcocite. According to the direct mechanism, the leaching microorganisms directly participate in the leaching reaction to accelerate the leaching of chalcocite, and the final leaching product is sulfate. The reactions are shown as follows [41]:

$$Cu_2S+2H^++0.5O_2 \xrightarrow{\text{Bacteria}} CuS+Cu^{2+}+H_2O \quad (9)$$

$$CuS+2O_2 \xrightarrow{\text{Bacteria}} CuSO_4 \quad (10)$$

However, the direct mechanism for chalcocite bioleaching has gradually been questioned with extensive investigations of the crystal structure and clarification of the chemical dissolution process of chalcocite.

The indirect mechanism indicates that leaching microorganisms accelerate the leaching of chalcocite by oxidizing Fe^{2+} to Fe^{3+} or oxidizing S^0 to sulfate instead of directly contributing to the dissolution of chalcocite, and the reactions are shown as follows [42]:

$$4Fe^{2+}+4H^++O_2 \xrightarrow{\text{Bacteria}} 4Fe^{3+}+2H_2O \quad (11)$$

$$S^0+H_2O+1.5O_2 \xrightarrow{\text{Bacteria}} 2H^++SO_4^{2-} \quad (12)$$

$$K^++3Fe^{3+}+2SO_4^{2-}+6H_2O \xrightarrow{\text{Bacteria}} KFe_3(SO_4)_2(OH)_6+6H^+ \quad (13)$$

The indirect mechanism for chalcocite bioleaching is commonly acknowledged to occur via chemical dissolution. CHENG [43] used SEM and XPS analyses and found that the surface of the chalcocite leaching residue was mostly composed of S^0 and jarosite, and similar results were also reported by other researchers [28,34,44]. In addition, the final oxidation product of secondary chalcocite produced by chalcopyrite bioleaching was also jarosite [45,46]. BOLORUNDURO [24] found that S^0 and sulfate were reaction products of the second stage chalcocite leaching at ambient temperature, and S^0 was produced prior to sulfate. Especially when the copper extraction level reached 70%, a large amount of S^0 accumulated on the mineral surface to prevent further dissolution of the chalcocite. Afterward, iron-oxidizing bacteria increased the redox potential by oxidizing Fe^{2+} to Fe^{3+}, while sulfur-oxidizing bacteria improved the leaching rate by oxidizing S^0 directly. However, the structure of the coated S^0 became loose and porous when the leaching temperature was above 75 °C, which enabled further bioleaching of the chalcocite. Through SEM−EDS, FTIR, and XRD analyses of the products on the mineral surface, BAMPOLE et al [47] also suggested that the indirect mechanism was the dominant leaching mechanism for the bioleaching process of mixed chalcopyrite−chalcocite.

According to WU et al [38], the largest barrier to oxidative dissolution of chalcocite was the formation of significant amounts of Cu_nS and S^0, which were coated on the mineral surface and reduced the electron transport rate. However, in the presence of leaching microorganisms, the hole concentration and solution potential increased due to the oxidation of Fe^{2+}, and the impedance arc decreased, which promoted the oxidation of Cu_nS and the S^0 passivation layer, thereby accelerating the dissolution of chalcocite. PHYO [48] clarified the role of microorganisms in enhancing chalcocite leaching. In addition to maintaining the potential balance, acidophilic iron-oxidizing bacteria were important in improving the diffusion driving force of Fe^{3+} and Fe^{2+}, while acidophilic sulfur-oxidizing bacteria were involved in the oxidation of the S^0 layer to reduce the diffusion barrier.

FENG et al [49] revealed that iron–sulfur

metabolism during chalcocite bioleaching can be promoted simultaneously by the addition of pyrite and sulfur oxidizing bacteria, and the underlying mechanism is shown in Fig. 3. Numerous particles and corrosion traces were generated on the ore surface, and the biomass concentration was increased to 2.19×10^7 cells/mL, indicating a strong relationship between minerals and microorganisms. Moreover, confocal laser scanning microscopy (CLSM) also indicated the accumulation of cells and extracellular polymers (EPS) on the ore surface, which suggested strong contact leaching mechanism [50].

Besides, aeration with CO_2 and N_2 was reported to have a significant effect on the composition of the microbial community in column bioleaching of chalcocite. Oxygen limitations altered the microbial communities during the bioleaching, but aeration with CO_2 and N_2 enabled the growth of sulfur-oxidizing bacteria and iron-oxidizing bacteria and was used to adjust the role of microorganisms in mineral bioleaching [51]. Moreover, the concentration of Cu^{2+} also had an effect on chalcocite bioleaching. It was reported that the leaching process of high-grade chalcocite was strengthened if the leaching solution was extracted in a timely manner when the Cu^{2+} concentration was greater than 3.5g/L [52].

4 Leaching kinetics of chalcocite

The leaching kinetics of chalcocite can be divided into two distinct stages. In the first stage, a portion of the Cu^{2+} is released, and the resulting chalcocite is gradually transformed into covellite. In the second stage, the covellite continues to release Cu^{2+} and produces S^0. The interatomic valence bond structure of chalcocite is more easily destroyed due to its low lattice energy, whereas the crystal structure of secondary covellite is more resistant to destruction due to its high lattice energy.

The Cu^+ in the chalcocite crystals was well diffused as quickly as it did in aqueous solution. Therefore, crystalline Cu^+ was rapidly transferred to the mineral surface and oxidized to Cu^{2+} in the first stage of chalcocite leaching. The dissolution process was divided into three steps, as shown in Reactions (14)−(16) [34].

In the first step, the Cu^+ in the chalcocite crystals moved to the surface, and unstable covellite ($Cu^{2+}S^{2-}$) and ionic holes (V_{Cu^+}) were generated in the crystals:

$$(Cu^+)_2S^{2-}\rightarrow Cu^{2+}S^{2-}+V_{Cu^+}+Cu^+ \quad (14)$$

In the second step, the unstable covellite ($Cu^{2+}S^{2-}$) was converted into structurally stable covellite ($(Cu^+)_2S_2^{2-}$):

$$Cu^{2+}S^{2-}\rightarrow 0.5(Cu^+)_2S_2^{2-} \quad (15)$$

In the third step, the Cu^+ on the surface was oxidized to Cu^{2+} and dissolved in the solution:

$$Cu^++Fe^{3+}\rightarrow Fe^{2+}+Cu^{2+} \quad (16)$$

However, in the second stage of chalcocite leaching, the Cu^+ in the covellite crystals cannot

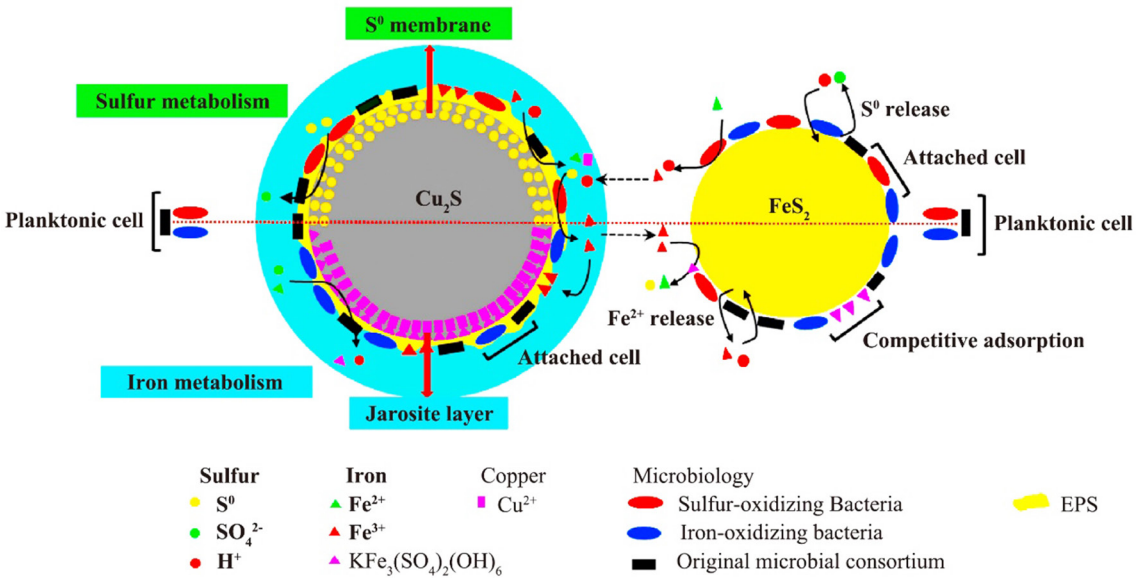

Fig. 3 Bioleaching mechanism of chalcocite in presence of pyrite, sulfur-oxidizing bacteria, and iron-oxidizing bacteria [49]

move quickly enough to the mineral surface and undergo oxidation to Cu^{2+} due to its slow diffusion rate. Therefore, the dissolution rate in the second stage was significantly slower than that in the first stage.

In general, the dissolution kinetics for the first stage leaching of chalcocite is considered to be controlled by the diffusion of oxidants with a moderate activation energy (4−30 kJ/mol) [27,53]. Table 1 gives the activation energy and kinetic control model for the first stage of chalcocite leaching.

However, the dissolution kinetics for the second stage of chalcocite leaching is significantly different from that of the first stage, which is controlled by chemical reactions, electrochemical or product layer diffusion [24,27,56]. The activation energy is greater (55−105 kJ/mol), and the leaching rate is sensitive to the leaching temperature [57,58]. In addition, secondary covellite is more soluble than natural covellite [53,56]. Table 2 gives the activation energy and kinetic control model for the second stage of chalcocite leaching.

4.1 Effect of temperature

The effect of temperature on the leaching rate of chalcocite is depended on the activation energy. Due to its low activation energy, leaching during the first stage was fast even at room temperature. However, leaching in the second stage was relatively low and was strongly affected by temperature due to the high activation energy.

The leaching kinetics of the second stage may indicate a dual mechanism. At temperatures below 60 °C, the leaching rate was controlled by chemical reactions, whereas it was controlled by diffusion at temperatures above 60 °C [55].

In addition, RUAN [34] systematically studied the leaching progress of digenite in the Zijinshan Copper Mine (China); it was found that the copper

Table 1 Activation energy and kinetic control model for first stage of chalcocite leaching

Mineral	Temperature/°C	Activation energy/(kJ·mol^{-1})	Mechanism	Ref.
Synthetic Cu_2S	30−60	6.3	Diffusion control	[54]
Synthetic Cu_2S	60−90	22.2	Mixed control model	[54]
Synthetic Cu_2S	5−80	5−6	Diffusion control	[55]
Natural Cu_2S	30−90	11.7	Mixed control model	[34]
Natural Cu_2S	28−70	28.0	Diffusion control	[53]
Natural Cu_2S	35−75	34.0	Mixed control model	[24]
Natural Cu_2S	65−94	33.5	Diffusion control	[53]

Table 2 Activation energy and kinetic control model for second stage of chalcocite leaching

Mineral	Temperature/°C	Activation energy/(kJ·mol^{-1})	Mechanism	Ref.
Synthetic CuS	<60	92.1	Chemical reaction control	[55]
Synthetic CuS	60−80	33.5	Mixed control model	[55]
Synthetic CuS	30−90	83.7	Chemical reaction control	[54]
Synthetic CuS	15−95	75.3	Chemical reaction control	[34]
Natural Cu_2S	40−70	58.6	Chemical reaction control	[34]
Natural Cu_2S	30−90	75.3	Electrochemical control	[34]
Natural Cu_2S	35−75	96.3	Electrochemical control	[24]
Natural Cu_2S	75−95	69.0	Chemical reaction control (initial stage); Mixed control model (later stage)	[53]
Synthetic CuS	25−45	72.0	Chemical reaction control	[26]
Natural Cu_2S	25−60	80.8	Chemical reaction control (initial stage); Diffusion through product layer (later stage)	[28]
Natural Cu_2S	30−75	65.02	Chemical reaction control	[59]

extraction exceeded 40% after only 2 min of leaching at temperatures above 30 °C, and temperature had little effect on the first stage leaching of digenite. However, leaching in the second stage was relatively slow and significantly affected by the leaching temperature. It needed 12 h for copper extraction to increase from 40% to 45% at 30 °C, but when the leaching temperature was increased to 75 °C, the digenite was almost completely dissolved after 3 h of leaching.

WU [44] reported that temperature had the highest correlation index with the kinetic equation for dissolution of chalcocite, while other factors had little effect on the leaching process. With column leaching experiments, NIU et al [28] revealed that temperature affected the leaching kinetics by modifying the morphology of the S^0 coating, and the effect of temperature on chalcocite dissolution is shown in Fig. 4.

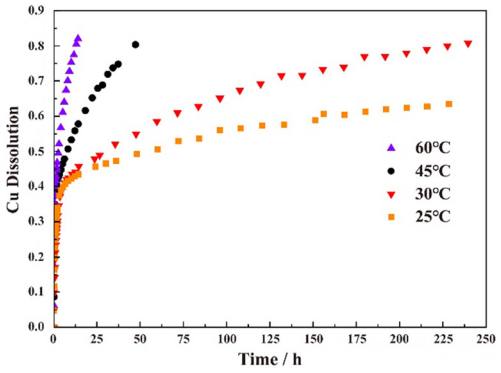

Fig. 4 Effect of temperature on chalcocite dissolution [28]

4.2 Effect of pH

For the two chalcocite leaching stages (Reactions (4) and (5)), H^+ is involved if oxygen is employed as an oxidant. Consequently, the leaching process is significantly influenced by the pH, with a lower pH resulting in a higher leaching rate.

However, H^+ is not directly involved in the oxidation reaction when ferric ions are used as the oxidant (Reactions (6) and (7)), which may have no effect on the leaching of chalcocite. THOMAS et al [55] confirmed this result, suggesting that the dissolution rate of chalcocite was independent of the pH when the ferric concentration was kept in the range 0.03−0.3 mol/L and that H^+ prevented the precipitation of Fe^{3+}. However, according to Reaction (8), H^+ is essential for Fe^{3+} regeneration, so a lower pH should be maintained to ensure cyclic regeneration of the Fe^{3+}. Additionally, additional acid is required if the ore contains significant amounts of alkaline minerals.

4.3 Effect of ferric concentration

Ferric ions are often used as oxidants for chalcocite dissolution due to their cheapness and feasibility. Due to the low lattice energy of chalcocite, a lower ferric acid concentration meets the requirement for the first stage of chalcocite leaching. As a result, the first stage of chalcocite leaching was not significantly affected by the ferric concentration at a certain point [54,55]. However, ferric ions may have a significant impact on the crystalline of intermediates. The crystallite size of the intermediate was smaller in the presence of ferric ions, which facilitated the rapid leaching of chalcocite [60].

Nevertheless, the effect of the ferric concentration on the second stage of chalcocite leaching is controversial. The leaching rate in the second stage was positively correlated with the ferric concentration when it was higher than 0.61 mol/L, and the kinetic correlation index of the ferric concentration was 0.3 [34]. However, other reports have suggested that when the ferric concentration was higher than 0.005 mol/L or even 0.3 mol/L, leaching rate during the second stage had litter relationship with the ferric concentration [55]. Moreover, NIU et al [28] found that the ferric concentration had little effect on the leaching kinetics of chalcocite (Fig. 5).

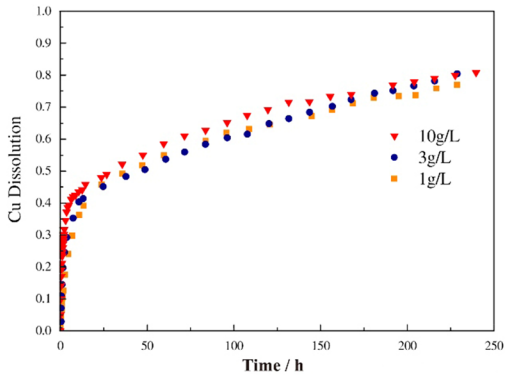

Fig. 5 Effect of ferric concentration on chalcocite dissolution [28]

4.4 Effect of redox potential

The present work indicates that the redox potential may have an important effect on the dissolution of chalcocite. BOLORUNDURO [24] researched the leaching kinetics of chalcocite at

redox potentials ranging from 531 to 567 mV (vs SHE). Although a variety of nonstoichiometric copper−sulfur compounds appeared during the first stage of leaching, the redox potential did not have a significant effect on the leaching rate. However, the dissolution rate during the second stage was significantly promoted when the redox potential was maintained at a relatively high level.

MIKI et al [26] explored the leaching kinetics of synthetic covellite, chalcocite and digenite at different redox potentials. The results showed that the leaching rate of covellite at 839 mV (vs SHE) was similar to that at 889 mV (vs SHE). However, the leaching rate significantly decreased when the redox potential was reduced to 789 mV (vs SHE). Moreover, for chalcocite or digenite, leaching in the first stage was very fast at a redox potential of 739 mV (vs SHE), but it decreased significantly when the copper extraction reached 50% (Cu_2S) or 45% ($Cu_{1.8}S$). However, the leaching rate of secondary covellite was significantly accelerated when the redox potential was increased to 789 mV (vs SHE) (Fig. 6).

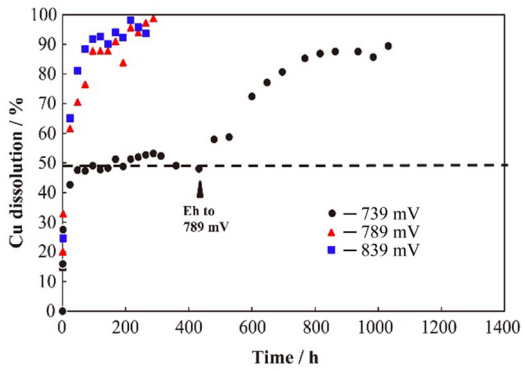

Fig. 6 Effect of redox potential on chalcocite dissolution [26]

In addition, RUAN [34] proposed that the redox potential had little effect on the rate of digenite dissolution when the leaching temperature was above 60 °C and the ferric concentration was above 0.1 mol/L, and the leaching temperature was suggested to be the most important factor for the dissolution of digenite.

4.5 Effect of particle sizes

It is generally accepted that the particle size has an important influence on chalcocite leaching [24]. HASHEMZADEH et al [61] reported that the particle size only affected the first stage of chalcocite leaching, and the effect was significantly reduced in the second stage due to the influence of the interfacial reaction area. However, some reports have suggested that the rate of chalcocite leaching was independent of the particle size [62,63].

PHYO et al [64] researched the effects of particle sizes on column leaching of chalcocite. Leaching of the large particles (31−200 mm) was very slow and there was no inflection point typically seen for leaching of small particles (0.054−31 mm). At Fe^{3+} concentration of 0.25 mol/L, a pH of 1.54, an E_h of 664 mV (vs SHE), and a temperature of 35 °C, the copper extraction reached 25% after 50 d of leaching for 90−200 mm chalcocite particles, but the copper extraction reached 75% for 3.5−9.5 mm particles. In addition, in the first stage of leaching (<45% dissolution), the effect of particle size on the dissolution of large particles was more pronounced than that on the dissolution of small particles, but the dissolution rate was not significantly affected by particle sizes in the second stage (>45% dissolution).

5 Industrial application of chalcocite leaching

Originating from acid leaching of copper oxide minerals, the industrial practice of chalcocite heap leaching has been practiced for several decades. The Lo Aguirre Mine in Chile was the first mine to adopt the industrial practice of heap bioleaching in 1980. Since the 1990s, heap bioleaching has been employed at numerous chalcocite mines for extracting copper [65]. Part of the mines that achieved the industrial practice of chalcocite heap bioleaching are given in Table 3.

In terms of the copper produced and revenue generated, chalcocite heap bioleaching is the largest industrial application of bioleaching. Figure 7 presents a simplified schematic showing the solution management and heap aeration methods used for chalcocite heap leaching [68]. Although this seems to be a fairly straightforward process in theory, chalcocite heap bioleaching is a fairly complicated process in practice. DIXON and PETERSEN [73] suggested that with leachate trickles, four subprocesses ranging from the macro- to the microscale occurred simultaneously within the ore bed.

Table 3 Part of mines that achieved industrial practice of chalcocite heap bioleaching

Country	Mine	Operating period	Reserve/kt	Copper grade/%	Ore processed/(kt·d^{-1})	Ref.
Chile	Lo Aguirre	1980−1996	12000	1.5	16	[66]
Chile	Cerro Colorado	1993−	80000	1.4	16	[67]
Chile	Ivan Zar	1994−	5000	2.5	1.5	[34]
Chile	Quebrada Blanca	1994−	85000	1.4	17.3	[65]
Chile	Andacollo	1996−	32000	0.58	15	[34]
Chile	Dos Amigos	1996−	−	2.5	3	[68]
Chile	Zaldivar	1995−	120000	1.4	20	[69]
USA	Morenci	2001−	3450000	0.28	75	[70]
Australia	Gunpowder Mammoth	1991−	1200	1.8	−	[65]
Australia	Girilambone	1993−2003	8000	2.4	2	[34]
Australia	Nitty Copper	1998−	−	1.2	5	[68]
Australia	Mt Leyshon	1992−1997	−	0.15	1.3	[68]
Myanmar	Monywa	1999−	126000	0.5	18	[71]
China	Zijinshan	2005−	400000	0.43	15	[27,64]
China	Jinchuan	2006−	240000	0.65	−	[72]

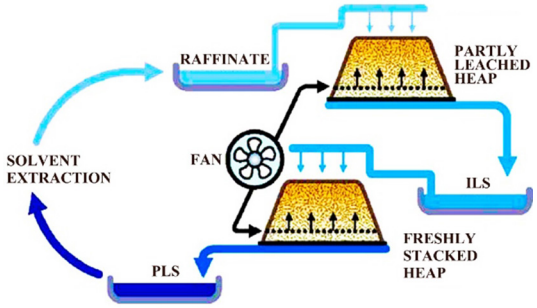

Fig. 7 Simplified schematic of solution management and heap aeration for chalcocite heap leaching [68]

During heap leaching, it is beneficial to pumping sufficient air into the heap to satisfy the physiological requirements of the bacteria and optimize the bacterial activity, thus facilitating the leaching of chalcopyrite. This practice has been proven to be effective by heap leaching plants in Chile and Australia [68]. Based on the culture-independent PCR-DGGE analytical technique for the 16S rRNA gene, HAWKES et al [74] researched the microbiology of the heap bioleaching of MICCL Monywa chalcocite. Six strains were isolated, including a new archaea "*Ferroplasma Cupricumulans*". The microbial community produced by Myanmar bioleaching contained more biomass, and the operating parameters of the Myanmar reactor enabled the growth of moderately thermophilic microorganisms.

LEAHY et al [75] proposed a three-phase computational hydrodynamics model to understand thermodynamics of chalcocite heap bioleaching. The results showed that the concentration of leaching bacteria was related to the leaching temperature, and heap leaching worked in a top−down manner. Firstly, the top part of the heap was cooled with the addition of new leachate, which encouraged the growth of leaching bacteria and accelerated bioleaching of the chalcocite. Afterward, as the top part was completely leached, the leaching front moved down and gradually leached the entire heap.

However, chalcocite heap leaching is a complex system in practice, and it is not appropriate to focus on specific subprocesses in isolation. Instead, the potential for heap leaching should be fully exploited by building holistic models to explain the interactions among these processes. The Phelps Dodge (PD) copper stockpile model [76] and the CSIRO Heap model [58] are typical multidimensional models used to simulate the spatial structures of leaching reactors. The PD model has the ability to simulate leaching conditions within an individual lift, while the CSIRO model is usually used to research local structures associated with individual air distributors and acid droplets. In addition, the two models have the ability to simulate both the gas and liquid

phases simultaneously.

PETERSEN and DIXON [57] employed the comprehensive modeling tool HeapSim to reveal the interactions between the scales of chalcocite grains, particles, clusters and the whole heap. It was found that even at ambient temperature, higher copper extraction can be achieved within a few months under optimized conditions in theory. However, copper extraction in industrial chalcocite heap bioleaching actually was depended on two major factors. One was the poor distribution of reagents in the heap due to the patterns of local flow and stagnant solutions, and the other was the low microbial activity attributed to unfavorable solution chemistry and limited CO_2 supplementation. The effects of these two factors on the overall rate-limiting effect of copper extraction were approximately of the same magnitude.

In conclusion, although the industrial practice of chalcocite heap bioleaching has been applied successfully for several decades, the leaching rates and copper extraction requirements are unsatisfactory, which limits rapid development and industrial application of chalcocite bioleaching.

6 Application of synchrotron radiation-based research methods

Synchrotron radiation (SR) is electromagnetic radiation emitted by relativistically charged particles traveling along curved orbits due to the effect of an electromagnetic field. Compared with traditional light sources, synchrotron radiation has many advantages and is currently one of the most effective light sources in the world. Synchrotron radiation can be used to conduct a wide range of cutting-edge scientific investigations that are not possible with traditional light sources. At present, there are many experimental techniques based on synchrotron radiation, including infrared spectroscopy, microscopic imaging, X-ray diffraction, X-ray photoelectron spectroscopy, mass spectrometry, and X-ray absorption spectroscopy. Additionally, these methods have seen widespread application in many frontier research fields such as pharmaceutical science, environmental science, chemistry, mineralogy, metallurgy and geology [39,77−80].

SR-based research methods have been used to explore the chemical−biological leaching mechanism of copper sulfide minerals. LIU et al [81,82] established a database of K-edge XANES absorption spectra of S and L-edge XANES absorption spectra of Fe for various standard substances containing S, Fe, and Cu. SR-XRD and XANES were employed to research the phase transitions and element migration processes on the chalcopyrite surface in a typical bioleaching system. When the potential was less than 871 mV (vs SHE), bornite and chalcocite appeared as intermediates on days 3 and 9, respectively. However, the bornite and chalcocite disappeared successively and were eventually transformed into covellite when the potential was increased above 921 mV (vs SHE). By linear fitting of the XANES spectrum, it was found that the relative content of each intermediate component changed continuously with increasing leaching time, during which the redox potential played an important role.

Additionally, YANG et al [83,84] combined electrochemical methods with SR-based equipment and examined the surface chemical substances formed during the chalcopyrite bioleaching process for different leaching bacteria. FANG et al [85] and WANG et al [86] employed SR-XRD to study the fine phase transformations of chalcocite leaching in an acidic ferric sulfate solution and the synergistic leaching mechanism of bornite and pyrite. BEATTIE et al [87], ACRES et al [88], and MAJUSTE et al [89] conducted a series of SR-XPS, NEXAFS and SR-XRD tests on the leaching residues of copper sulfide minerals. The variations on the mineral surfaces were characterized for different concentrations of KOH or H_2SO_4, and the leaching mechanisms were clarified.

7 Conclusions

(1) Due to its high copper content and easily leached crystal structure, chalcocite is one of the most valuable minerals for industrial copper extraction. The process of chalcocite dissolution follows the paths of polysulfur compounds, and CuS and S^0 are significant intermediate products. The bioleaching of chalcocite is generally thought to be an indirect mechanism, and leaching micro-organisms accelerate the leaching of chalcocite mostly by oxidizing Fe^{2+} to Fe^{3+} or helping to oxidize the coating S^0. The first stage of chalcocite leaching has a lower activation energy and is controlled by the diffusion of oxidants, while the

second stage has a higher activation energy and is controlled by chemical reaction, electrochemistry or product layer diffusion. The interactions between subprocess of chalcocite industrial heap bioleaching are complex, and the distribution of reagents and the activity of the microorganisms play important roles.

(2) In the future, several advanced research methods, including synchrotron radiation, should be introduced to explore the chemical−biological dissolution mechanism and leaching kinetics of chalcocite. In addition, special attention should be paid to key issues in industrial-scale bioleaching, and these issues may directly improve the leaching efficiency of chalcocite.

CRediT authorship contribution statement

Chao-jun FANG: Software, Formal analysis, Investigation, Data curation, Writing − Original draft, Visualization, Project administration, Funding acquisition; **Jun WANG:** Methodology, Validation, Resources, Writing − Review & editing, Funding acquisition; **Guan-zhou QIU:** Conceptualization, Supervision, Funding acquisition.

Declaration of competing interest

The authors declare that they have no known competing financial interests or personal relationships that could have appeared to influence the work reported in this paper.

Acknowledgments

This research was funded by the National Natural Science Foundation of China (Nos. 52004086, 52274288, 51934009), National Key Research and Development Plan of China (No. 2022YFC2105300), China Postdoctoral Science Foundation (No. 2021M703620), the Key Project of Science and Technology of Henan Province, China (No. 202102310543), the Key Research Project of Colleges and Universities in Henan Province, China (No. 21A440007), the Open Foundation of State Key Laboratory of Complex Nonferrous Metal Resources Clean Utilization, China (No. CNMRCUKF2009), and the Natural Science Foundation of Henan Polytechnic University, China (No. B2020-27).

References

[1] BAI Y L, WANG W, XIE F, LU D K, JIANG K X. Effect of temperature, oxygen partial pressure and calcium lignosulphonate on chalcopyrite dissolution in sulfuric acid solution [J]. Transactions of Nonferrous Metals Society of China, 2022, 32: 1650−1663.

[2] YANG C R, JIAO F, QIN W Q. Leaching of chalcopyrite: An emphasis on effect of copper and iron ions [J]. Journal of Central South University, 2018, 25: 2380−2386.

[3] YANG Y, ZHU Z Y, HU T T, ZHANG M J, QIU G Z. Variation in energy metabolism structure of microbial community during bioleaching chalcopyrites with different iron-sulfur ratios [J]. Journal of Central South University, 2021, 28: 2022−2036.

[4] WU A X, HU K J, WANG H J, ZHANG A Q, YANG Y. Effect of ultraviolet mutagenesis on heterotrophic strain mutation and bioleaching of low grade copper ore [J]. Journal of Central South University, 2017, 24: 2245−2252.

[5] QIU G Z, LIU X D. Biotech key to unlock mineral resources value [J]. Transactions of Nonferrous Metals Society of China, 2022, 32: 2309−2317.

[6] CHANG K X, ZHANG Y S, ZHANG J M, LI T F, WANG J, QIN W Q. Effect of temperature-induced phase transitions on bioleaching of chalcopyrite [J]. Transactions of Nonferrous Metals Society of China, 2019, 29: 2183−2191.

[7] BRIERLEY C L, BRIERLEY J A. Progress in bioleaching. Part B: Applications of microbial processes by the minerals industries [J]. Applied Microbiology and Biotechnology, 2013, 97: 7543−7552.

[8] BRIERLEY J A, BRIERLEY C L. Present and future commercial applications of biohydrometallurgy [J]. Hydrometallurgy, 2001, 59: 233−239.

[9] ZHAO C X, YANG B J, WANG X X, ZHAO H B, GAN M, QIU G Z, WANG J. Catalytic effect of visible light and Cd^{2+} on chalcopyrite bioleaching [J]. Transactions of Nonferrous Metals Society of China, 2020, 30: 1078−1090.

[10] YANG C R, JIAO F, QIN W Q. Cu-state evolution during leaching of bornite at 50 °C [J]. Transactions of Nonferrous Metals Society of China, 2018, 28: 1632−1639.

[11] ZHU P, LIU X D, CHEN A J, LIU H W, YIN H Q, QIU G Z, HAO X D, LIANG Y L. Comparative study on chalcopyrite bioleaching with assistance of different carbon materials by mixed moderate thermophiles [J]. Transactions of Nonferrous Metals Society of China, 2019, 29: 1294−1303.

[12] NIE Z Y, ZHANG W W, LIU H C, ZHU H R, ZHAO C H, ZHANG D R, ZHU W, MA C Y, XIA J L. Bioleaching of chalcopyrite with different crystal phases by *Acidianus manzaensis* [J]. Transactions of Nonferrous Metals Society of China, 2019, 29: 617−624.

[13] WANG J, ZHU S, ZHANG Y S, ZHAO H B, HU M H, YANG C R, QIN W Q, QIU G Z. Bioleaching of low-grade copper sulfide ores by *Acidithiobacillus ferrooxidans* and *Acidithiobacillus thiooxidans* [J]. Journal of Central South University, 2014, 21: 728−734.

[14] LAN Z Y, HU Y H, LIU J S, WANG J. Solvent extraction of copper and zinc from bioleaching solutions with LIX984 and D2EHPA [J]. Journal of Central South University of Technology, 2005, 12: 45−49.

[15] DOMIC E M. A review of the development and current status of copper bioleaching operations in Chile: 25 years of successful commercial implementation [C]//RAWLINGS D E, JOHNSON D B. Biomining. Berlin, Heidelberg: Springer, 2007: 81−95.

[16] BUERGER M J, WUENSCH B J. Distribution of atoms in high chalcocite, Cu_2S [J]. Science, 1963, 141: 276−277.
[17] EVANS H T Jr. Djurleite ($Cu_{1.94}S$) and low chalcocite (Cu_2S): New crystal structure studies [J]. Science, 1979, 203: 356−358.
[18] EVANS H T. Copper coordination in low chalcocite and djurleite and other copper-rich sulfides [J]. American Mineralogist, 1981, 66: 807−818.
[19] WILL G, HINZE E, ABDELRAHMAN A R M. Crystal structure analysis and refinement of digenite, $Cu_{1.8}S$, in the temperature range 20 to 500 °C under controlled sulfur partial pressure [J]. European Journal of Mineralogy, 2002, 14: 591−598.
[20] EVANS H T. Crystal structure of low chalcocite [J]. Nature Physical Science, 1971, 232: 69−70.
[21] CRUNDWELL F K. The influence of the electronic structure of solids on the anodic dissolution and leaching of semiconducting sulphide minerals [J]. Hydrometallurgy, 1988, 21: 155−190.
[22] LU D K, JIANG K X, WANG C, LIU D X. Leaching mechanism of chalcocite and covellite [J]. Nonferrous Metals, 2002, 54: 31−35. (in Chinese)
[23] YANG X W, SHEN Q F, GUO Y X. Biohydrometallurgy [M]. Beijing: Metallurgical Industry Press, 2003. (in Chinese)
[24] BOLORUNDURO S A. Kinetics of leaching of chalcocite in acid ferric sulfate media: Chemical and bacterial leaching [D]. Vancouver, BC, Canada: The University of British Columbia, 1999.
[25] YU S C, LIAO R, YANG B J, FANG C J, WANG Z T, LIU Y L, WU B Q, WANG J, QIU G Z. Chalcocite (bio)hydrometallurgy—Current state, mechanism, and future directions: A review [J]. Chinese Journal of Chemical Engineering, 2022, 41, 109−120.
[26] MIKI H, NICOL M, VELÁSQUEZ-YÉVENES L. The kinetics of dissolution of synthetic covellite, chalcocite and digenite in dilute chloride solutions at ambient temperatures [J]. Hydrometallurgy, 2011, 105: 321−327.
[27] RUAN R M, ZOU G, ZHONG S P, WU Z L, CHAN B, WANG D Z. Why Zijinshan copper bioheapleaching plant works efficiently at low microbial activity — Study on leaching kinetics of copper sulfides and its implications [J]. Minerals Engineering, 2013, 48: 36−43.
[28] NIU X P, RUAN R M, TAN Q Y, JIA Y, SUN H Y. Study on the second stage of chalcocite leaching in column with redox potential control and its implications [J]. Hydrometallurgy, 2015, 155: 141−152.
[29] SCHIPPERS A, SAND W. Bacterial leaching of metal sulfides proceeds by two indirect mechanisms via thiosulfate or via polysulfides and sulfur [J]. Applied and Environmental Microbiology, 1999, 65: 319−321.
[30] WHITESIDE L S, GOBLE R J. Structural and compositional changes in copper sulfide during leaching and dissolution [J]. Canadian Mineralogist, 1986, 24: 247−258.
[31] HASHEMZADEH M, LIU W Y. The response of sulfur chemical state to different leaching conditions in chloride leaching of chalcocite [J]. Hydrometallurgy, 2020, 192: 105245.
[32] HIDALGO T, VERRALL M, BEINLICH A, KUHAR L, PUTNIS A. Replacement reactions of copper sulphides at moderate temperature in acidic solutions [J]. Ore Geology Reviews, 2020, 123: 103569.
[33] TORRES D, TRIGUEROS E, ROBLES P, LEIVA W H, JELDRES R I, TOLEDO P G, TORO N. Leaching of pure chalcocite with reject brine and MnO_2 from manganese nodules [J]. Metals, 2020, 10: 1426.
[34] RUAN R M. A case study on bio-heapleaching practice of Zijinshan copper sulphide: Kinetics and process optimization [D]. Changsha: Central South University, 2011. (in Chinese)
[35] ARCE E M, GONZÁLEZ I. A comparative study of electrochemical behavior of chalcopyrite, chalcocite and bornite in sulfuric acid solution [J]. International Journal of Mineral Processing, 2002, 67: 17−28.
[36] ELSHERIEF A E, SABA A E, AFIFI S E. Anodic leaching of chalcocite with periodic cathodic reduction [J]. Minerals Engineering, 1995, 8: 967−978.
[37] WEN J K. Research and application on selective bioleaching of high sulfur low copper secondary copper sulfide ore [D]. Beijing: General Research Institute for Nonferrous Metals, 2016. (in Chinese)
[38] WU B, LIAO B, LIU X, WEN J K. A study on electrochemical fundamentals and kinetics of bioleaching of chalcocite [J]. Chinese Journal of Rare Metals, 2019, 43(12): 1332−1337. (in Chinese)
[39] TODD E C, SHERMAN D M. Surface oxidation of chalcocite (Cu_2S) under aqueous (pH=2−11) and ambient atmospheric conditions: Mineralogy from Cu L- and O K-edge X-ray absorption spectroscopy [J]. American Mineralogist, 2003, 88: 1652−1656.
[40] VELÁSQUEZ P, LEINEN D, PASCUAL J, RAMOS-BARRADO J R, CORDOVA R, GÓMEZ H, SCHREBLER R. XPS, SEM, EDX and EIS study of an electrochemically modified electrode surface of natural chalcocite (Cu_2S) [J]. Journal of Electroanalytical Chemistry, 2001, 510: 20−28.
[41] SAKAGUCHI H, TORMA A E, SILVER M. Microbiological oxidation of synthetic chalcocite and covellite by *Thiobacillus ferrooxidans* [J]. Applied and Environmental Microbiology, 1976, 31: 7−10.
[42] MANCHISI J, HANSFORD G, GAYLARDI P, SIMUKANGA S, NYIRENDA R L, SICHALWE A. Potential for bioleaching copper sulphide rougher concentrates of Nchanga Mine, Chingola, Zambia [J]. Journal of the South African Institute of Mining and Metallurgy, 2012, 112: 1051−1058.
[43] CHENG H N. Bioleaching and mechanism of anilite, covellite and chalcopyrite [D]. Changsha: Central South University, 2010. (in Chinese)
[44] WU B. A study on fundamentals of selective inhibit pyrite bioleaching of chalcocite and covelite [D]. Beijing: General Research Institute for Nonferrous Metals, 2017. (in Chinese)
[45] WU S F, YANG C R, QIN W Q, JIAO F, WANG J, ZHANG Y S. Sulfur composition on surface of chalcopyrite during its bioleaching at 50 °C [J]. Transactions of Nonferrous Metals Society of China, 2015, 25: 4110−4118.
[46] LIU H C, XIA J L, NIE Z Y, WEN W, YANG Y, MA C Y, ZHENG L, ZHAO Y D. Formation and evolution of secondary minerals during bioleaching of chalcopyrite by

thermoacidophilic Archaea *Acidianus manzaensis* [J]. Transactions of Nonferrous Metals Society of China, 2016, 26: 2485−2494.

[47] BAMPOLE D L, LUIS P, MULABA-BAFUBIANDI A F. Sustainable copper extraction from mixed chalcopyrite–chalcocite using biomass [J]. Transactions of Nonferrous Metals Society of China, 2019, 29: 2170−2182.

[48] PHYO H A. Study on the effect of particle size on chalcocite dissolution kinetics under controlled E_h in chemical and bacterial leaching [D]. Beijing: Institute of Process Engineering, Chinese Academy of Sciences, 2020. (in Chinese)

[49] FENG S S, YIN Y J, YIN Z W, ZHANG H L, ZHU D Q, TONG Y J, YANG H L. Simultaneously enhance iron/sulfur metabolism in column bioleaching of chalcocite by pyrite and sulfur oxidizers based on joint utilization of waste resource [J]. Environmental Research, 2021, 194: 110702.

[50] HONG X J. Utilization of low-grade chalcocite with acidophilic iron oxidizing/reducing bacteria via bioleaching [D]. Wuxi: Jiangnan University, 2021. (in Chinese)

[51] CHEN B W, WU B, LIU X Y, WEN J K. Effect of CO_2 and N_2 on microbial community changes during column bioleaching of low-grade high pyrite-bearing chalcocite ore [J]. Journal of Central South University, 2015, 22: 4528−4535.

[52] YANG J L, XU J Y, ZHONG C G, LIANG X X, ZHAO S G, LIU Y F, ZHANG L H. A method for strengthening the extraction of copper in high-grade chalcocite: CN Patent, 112626336 [P]. 2020−12−11. (in Chinese)

[53] CHENG C Y, LAWSON F. The kinetics of leaching chalcocite in acidic oxygenated sulphate-chloride solutions [J]. Hydrometallurgy, 1991, 27: 249−268.

[54] WANDZILAK P, ADAMCZYK Z. Kinetics of cuprous sulphide leaching in acidic solutions [J]. Hydrometallurgy, 1993, 34: 13−22.

[55] THOMAS G, INGRAHAM T R, MACDONALD R J C. Kinetics of dissolution of synthetic digenite and chalcocite in aqueous acidic ferric sulphate solutions [J]. Canadian Metallurgical Quarterly, 1967, 6: 281−292.

[56] CHENG C Y, LAWSON F. The kinetics of leaching covellite in acidic oxygenated sulphate-chloride solutions [J]. Hydrometallurgy, 1991, 27: 269−284.

[57] PETERSEN J, DIXON D G. Principles, mechanisms and dynamics of chalcocite heap bioleaching [C]//DONATI E R, SAND W. Microbial Processing of Metal Sulfides. Berlin: Springer, 2007: 193−218.

[58] LEAHY M J, DAVIDSON M R, SCHWARZ M P. A model for heap bioleaching of chalcocite with heat balance: Mesophiles and moderate thermophiles [J]. Hydrometallurgy, 2007, 85: 24−41.

[59] SHANG H, GAO W C, WU B, WEN J K. Bioleaching and dissolution kinetics of pyrite, chalcocite and covellite [J]. Journal of Central South University, 2021, 28: 2037−2051.

[60] FANG C J, CAI T R, YU S C, GAO L J, HUANG L Y, PENG H, QIU G Z, WANG J. How ferric salt enhances the first-stage acidic leaching of chalcocite: Performance of intermediate crystallite [J]. JOM, 2022, 74: 1969−1977.

[61] HASHEMZADEH M, DIXON D G, LIU W Y. Modelling the kinetics of chalcocite leaching in acidified ferric chloride media under fully controlled pH and potential [J]. Hydrometallurgy, 2019, 186: 275−283.

[62] MAZUELOS A, PALENCIA I, ROMERO R, RODRÍGUEZ G, CARRANZA F. Ferric iron production in packed bed bioreactors: influence of pH, temperature, particle size, bacterial support material and type of air distributor [J]. Minerals Engineering, 2001, 14: 507−514.

[63] DEVECI H. Effect of particle size and shape of solids on the viability of acidophilic bacteria during mixing in stirred tank reactors [J]. Hydrometallurgy, 2004, 71: 385−396.

[64] PHYO H A, JIA Y, TAN Q Y, ZHAO S G, LIANG X X, RUAN R M, NIU X P. Effect of particle size on chalcocite dissolution kinetics in column leaching under controlled Eh and its implications [J]. Physicochemical Problems of Mineral Processing, 2020, 56: 676−692.

[65] RAWLINGS D E, JOHNSON B D. Biomining [M]. Berlin: Springer, 2007.

[66] BUSTOS S, CASTRO S, MONTEALEGRE R. The sociedad minera pudahuel bacterial thin-layer leaching process at Lo Aguirre [J]. FEMS Microbiology Reviews, 1993, 11: 231−235.

[67] PEACEY J, GUO X J, ROBLES E. Copper hydrometallurgy: Current status, preliminary economics, future direction and positioning versus smelting [J]. Transactions of Nonferrous Metals Society of China, 2004, 14: 560−568.

[68] WATLING H R. The bioleaching of sulphide minerals with emphasis on copper sulphides — A review [J]. Hydrometallurgy, 2006, 84: 81−108.

[69] KODALI P, DEPCI T, DHAWAN N, WANG X M, LIN C L, MILLER J D. Evaluation of stucco binder for agglomeration in the heap leaching of copper ore [J]. Minerals Engineering, 2011, 24: 886−893.

[70] SCHUMER B N, STEGEN R J, BARTON M D, HISKEY J B, DOWNS R T. Mineralogical profile of supergene sulfide ore in the western copper area, Morenci mine, Arizona [J]. Canadian Mineralogist, 2019, 57(3): 391−401.

[71] SOE K, RUAN R M, JIA Y, TAN Q Y, WANG Z T, SHI J F, ZHONG C G, SUN H Y. Influence of jarosite precipitation on iron balance in heap bioleaching at Monywa copper mine [J]. Journal of Mining Institute, 2021, 247: 102−113.

[72] FANG Z H, CHEN Q J. Effect of technological factors on bacterial leaching of low-grade Ni−Cu sulfide ore [J]. Transactions of Nonferrous Metals Society of China, 2001, 11: 774−777.

[73] DIXON D G, PETERSEN J. Comprehensive modelling study of chalcocite column and heap bioleaching [C]//RIVEROS P A, DIXON D G, DREISINGER D B, MENACHO J M. Copper 2003−Hydrometallurgy of copper (Book 2). Santiago, Chile: CIM-MetSoc, 2003: 493−516.

[74] HAWKES R B, FRANZMANN P D, PLUMB J J. Moderate thermophiles including "*Ferroplasma cupricumulans*" sp. nov. dominate an industrial-scale chalcocite heap bioleaching operation [J]. Hydrometallurgy, 2006, 83: 229−236.

[75] LEAHY M J, DAVIDSON M R, SCHWARZ M P. A model for heap bioleaching of chalcocite with heat balance: Bacterial temperature dependence [J]. Minerals Engineering, 2005, 18: 1239−1252.

[76] BENNETT C, CROSS M, CROFT N, UHRIE J L, GREEN

C R, GEBHARDT J. A comprehensive copper stockpile leach model: Background and model formulation [C]//YOUNG C A, ALFANTAZI A M, ANDERSON C G, DREISINGER D B, HARRIS B, JAMES A. Hydrometallurgy 2003−Volume 1: Leaching and solution purification. Warrendale, USA: TMS, 2003: 315−328.

[77] FANG C J, YU S C, WEI X Y, PENG H, OU L M, ZHANG G F, WANG J. The cation effect on adsorption of surfactant in the froth flotation of low-grade diasporic bauxite [J]. Minerals Engineering, 2019, 144: 106051.

[78] THYREL M, BACKMAN R, THÅNELL K, KARUNAKARAN C, SKYLLBERG U, LESTANDER T A. Nanomapping and speciation of C and Ca in thermally treated lignocellulosic cell walls using scanning transmission X-ray microscopy and K-edge XANES [J]. Fuel, 2016, 167: 149−157.

[79] GERLIN F, ZUPPELLA P, CORSO A J, NARDELLO M, TESSAROLO E, BACCO D, PELIZZO M G. Stability and extreme ultraviolet photo-reduction of graphene during C−K-edge NEXAFS characterization [J]. Surface and Coatings Technology, 2016, 296: 211−215.

[80] LIU W H, MEI Y, ETSCHMANN B, GLENN M, MACRAE C M, SPINKS S C, RYAN C G, BRUGGER J, PATERSON D J. Germanium speciation in experimental and natural sphalerite: Implications for critical metal enrichment in hydrothermal Zn−Pb ores [J]. Geochimica et Cosmochimica Acta, 2023, 342: 198−214.

[81] LIU H C, XIA J L, NIE Z Y. Relatedness of Cu and Fe speciation to chalcopyrite bioleaching by *Acidithiobacillus ferrooxidans* [J]. Hydrometallurgy, 2015, 156: 40−46.

[82] LIU H C, XIA J L, NIE Z Y, ZHEN X J, ZHANG L J. Differential expression of extracellular thiol groups of moderately thermophilic *Sulfobacillus thermosulfidooxidans* and extremely thermophilic *Acidianus manzaensis* grown on S^0 and Fe^{2+} [J]. Archives of Microbiology, 2015, 197: 823−831.

[83] YANG Y, HARMER S, CHEN M. Synchrotron X-ray photoelectron spectroscopic study of the chalcopyrite leached by moderate thermophiles and mesophiles [J]. Minerals Engineering, 2014, 69: 185−195.

[84] YANG Y, LIU W H, BHARGAVA S K, ZENG W M, CHEN M. A XANES and XRD study of chalcopyrite bioleaching with pyrite [J]. Minerals Engineering, 2016, 89: 157−162.

[85] FANG C J, YU S C, WANG X X, ZHAO H B, QIN W Q, QIU G Z, WANG J. Synchrotron radiation XRD investigation of the fine phase transformation during synthetic chalcocite acidic ferric sulfate leaching [J]. Minerals, 2018, 8: 461.

[86] WANG X X, LIAO R, ZHAO H B, HONG M X, HUANG X T, PENG H, WEN W, QIN W Q, QIU G Z, HUANG C M, WANG J. Synergetic effect of pyrite on strengthening bornite bioleaching by *Leptospirillum ferriphilum* [J]. Hydrometallurgy, 2018, 176: 9−16.

[87] BEATTIE D A, KEMPSON I M, FAN L J, SKINNER W M. Synchrotron XPS studies of collector adsorption and co-adsorption on gold and gold: silver alloy surfaces [J]. International Journal of Mineral Processing, 2009, 92: 162−168.

[88] ACRES R G, HARMER S L, BEATTIE D A. Synchrotron XPS studies of solution exposed chalcopyrite, bornite, and heterogeneous chalcopyrite with bornite [J]. International Journal of Mineral Processing, 2010, 94: 43−51.

[89] MAJUSTE D, CIMINELLI V S T, ENG P J, OSSEO-ASARE K. Applications of in situ synchrotron XRD in hydrometallurgy: Literature review and investigation of chalcopyrite dissolution [J]. Hydrometallurgy, 2013, 131/132: 54−66.

辉铜矿化学–生物溶解机制及浸出动力学进展

房朝军[1,2,3]，王 军[4,5]，邱冠周[4,5]

1. 河南理工大学 化学化工学院，焦作 454000；
2. 河南理工大学 煤炭安全生产与清洁高效利用省部共建协同创新中心，焦作 454000;
3. 昆明理工大学 省部共建复杂有色金属资源清洁利用国家重点实验室，昆明 650093；
4. 中南大学 资源加工与生物工程学院，长沙 410083；
5. 中南大学 生物冶金教育部重点实验室，长沙 410083

摘 要：辉铜矿是最具生物冶金工业利用价值的含铜矿物之一，然而，其生物浸出效率仍有较大提升空间。为了更好地揭示辉铜矿的生物浸出过程，对辉铜矿化学−生物溶解机制和浸出动力学相关研究进展进行综述。系统阐述辉铜矿的晶体结构，总结辉铜矿的化学溶解机制、电化学溶解机制和生物溶解机制，讨论辉铜矿的浸出动力学以及不同浸出参数对辉铜矿浸出的影响，总结辉铜矿生物冶金在工业应用中存在的问题。尽管如此，辉铜矿生物浸出的精细过程和浸出机制仍有待进一步研究。未来可采用同步辐射等多种新型研究方法在化学−生物多学科交叉基础上探明次生硫化铜矿的精细氧化溶解机制，为辉铜矿高效环保提铜奠定基础。

关键词：辉铜矿；生物浸出；溶解机制；动力学；同步辐射

(Edited by Bing YANG)